

Onset of wavenumber bandgaps via alternating Willis coupling signs

Hasan B. Al Ba'ba'a

Department of Mechanical Engineering, Union College, Schenectady, NY 12308, USA
albabaah@union.edu

Abstract — This article introduces a methodology for inducing wavenumber bandgaps via alternating Willis coupling signs. A non-reciprocal wave equation of Willis-type is first considered, and its wave dispersion analyses are carried out via the transfer matrix method. By creating unit cells from two identical Willis-type elastic layers, yet with reversed Willis-coupling signs, a reciprocal band structure peculiarly emerges, although each layer exhibits non-reciprocity if considered individually. Wavenumber bandgaps open due to such unit cell configuration, and their width and limits are analytically quantified. Similarities between materials with reversed-sign Willis coupling and bi-layered phononic crystals are noted, followed by concluding remarks.

Keywords — Wavenumber bandgaps, Willis coupling, non-reciprocal waves, periodic structures, dispersion diagram.

Background and motivation

Consider a non-reciprocal wave equation, in the absence of external forces [1]:

$$\frac{\partial^2 u}{\partial t^2} + 2v_0 \frac{\partial^2 u}{\partial x \partial t} + (v_0^2 - c^2) \frac{\partial^2 u}{\partial x^2} = 0 \quad (1)$$

governing the longitudinal displacement $u(x, t)$ of an axially moving elastic rod, quantified along the axial dimension x at any instant of time t . The wave speed in the elastic medium $c = \sqrt{E/\rho}$ is a function of its density ρ and modulus of elasticity E . The elastic rod is assumed to have a constant cross-sectional area A . Besides being of gyroscopic nature [2], Equation (1) is also known as a Willis-type equation of motion, where v_0 symbolizes the Willis coupling coefficient [3, 4], equivalent to the rod's speed [1]. Non-reciprocity in Willis-type elastic media stems from the introduced momentum bias, as evident from the mixed derivative term in Equation (1).

To examine wave dispersion and understand periodic structures governed by Equation (1), a transfer matrix of a unit cell of length x is developed. To streamline the analysis, three non-dimensional quantities are introduced: (i) a normalized modulation speed $\nu = v_0/c$, (ii) non-dimensional length $\xi = x/\ell$, and (iii) a non-dimensional time $\tau = \omega_0 t$, with $\omega_0 = c(1 - \nu^2)/\ell$ and ℓ being an arbitrary length. Implementing the non-dimensional quantities modifies Equation (1) to:

$$(1 - \nu^2) \frac{\partial^2 u}{\partial \tau^2} + 2\nu \frac{\partial^2 u}{\partial \xi \partial \tau} - \frac{\partial^2 u}{\partial \xi^2} = 0 \quad (2)$$

Following the methodology in Ref. [1] and assuming $u(\xi, \tau) = \tilde{u}(\xi)e^{-i\Omega\tau}$, the following unit-cell's transfer matrix is developed,

$$\mathbf{T}(\nu) = e^{-i\nu\Omega\xi} \mathbf{Y}(\nu) \quad (3)$$

where the matrix $\mathbf{Y}(\nu)$, having a determinant of one, is given by:

$$\mathbf{Y}(\nu) = \begin{bmatrix} \cos(\Omega\xi) + i\nu \sin(\Omega\xi) & \frac{1}{k\Omega} \sin(\Omega\xi) \\ -(1 - \nu^2)k\Omega \sin(\Omega\xi) & \cos(\Omega\xi) - i\nu \sin(\Omega\xi) \end{bmatrix} \quad (4)$$

In Equations (3) and (4), $\Omega = \omega/\omega_0$ is a normalized version of the excitation frequency ω , $k = EA/\ell$ is the effective longitudinal stiffness of a rod segment of length ℓ , and $i = \sqrt{-1}$ is the imaginary unit. The derived transfer matrix $\mathbf{T}(\nu)$ relates the state vectors at the terminals of the unit cell according to $\mathbf{z}(\xi) = \mathbf{T}(\nu)\mathbf{z}(0)$, where the state vector $\mathbf{z}(\xi) = \{\tilde{u}(\xi) f(\xi)\}^T$ compiles the displacement $\tilde{u}(\xi)$ and internal force $f(\xi) = k\tilde{u}_\xi$ at a given terminal at distance ξ .

Despite the introduction of a momentum bias, I next show the linearity of the dispersion relation from analyzing the eigenvalues of transfer matrix $\mathbf{T}(\nu)$ in Equation (3) with $\xi = 1$. Computing the determinant of $|\mathbf{T}(\nu) - \lambda \mathbf{I}| = 0$, where λ is an eigenvalue and \mathbf{I} is a 2×2 identity matrix, the following solutions of λ are derived:

$$\lambda = e^{-i\nu\Omega} \left(\frac{\text{tr}(\mathbf{Y})}{2} \pm i \sqrt{1 - \left(\frac{\text{tr}(\mathbf{Y})}{2} \right)^2} \right) \quad (5)$$

If the eigenvalues are written as $\lambda = e^{iq}$, where q is a non-dimensional wavenumber, the driven-wave dispersion relation is developed from Equation (5) after executing a few mathematical manipulations:

$$q = q_s \pm \Omega \quad (6)$$

where $q_s = -\nu\Omega$ is a wavenumber *phase shift*, reminiscent of the phase shift observed in Willis monatomic lattices recently developed by the author [5]. As evident from Equation (6), and in agreement with the results obtained in Ref. [1], the dispersion relation remains linear, even with the presence of Willis coupling (or rod's motion). However, the slopes of the dispersion branches (i.e., group velocity) corresponding to forward-going and backward-going waves are unequal, indicative of non-reciprocal wave propagation, and the change in slope is governed by the normalized modulation speed ν .

An additional observation I note here is that the angle at which the linear dispersion skews relative to the frequency axis can be analytically quantified via a straightforward trigonometry. More specifically, a triangle is formulated via the phase shift

¹The present study limits the value of the normalized modulation speed to the range $\nu \in [0, 1)$ to avoid possible dynamical instabilities [1].

q_s and its corresponding frequency Ω as shown in Figure 1, from which the skew angle ϕ can be derived:

$$\phi = \tan^{-1}(\nu) \quad (7)$$

This skew angle ϕ grows non-linearly starting from $\nu = 0$, the reciprocal case, for which the triangle understandably collapses to a line. Note that, unlike the phase shift q_s , the angle ϕ is independent of the frequency Ω . A comparison between the reciprocal case ($\nu = 0$) and a non-reciprocal one ($\nu = -1/3$) is shown in Figure 1.

As detailed earlier, a homogeneous elastic rod with a single Willis coupling results in non-reciprocity. One might then wonder: What is the effect of having a periodic variation in Willis coupling? Unlike elastic periodic structures with frequency bandgaps, such as rods with variation in mechanical properties [6–8], beams with periodically mounted local resonators [9–11], periodic gyroscopic systems [12–15], tensegrity chains [16–18], granular microstructures [19–22], among others [23–25], this work establishes that a homogeneous elastic rod with periodic alternating signs of Willis coupling opens *wavenumber* bandgaps. The presented approach adds to typical methods for initiating wavenumber bandgaps, encompassing structural damping [26], temporal stiffness modulation [27], supersonic spatiotemporal modulation [1], and the use of generally complex spatiotemporal harmonic functions for stiffness [28].

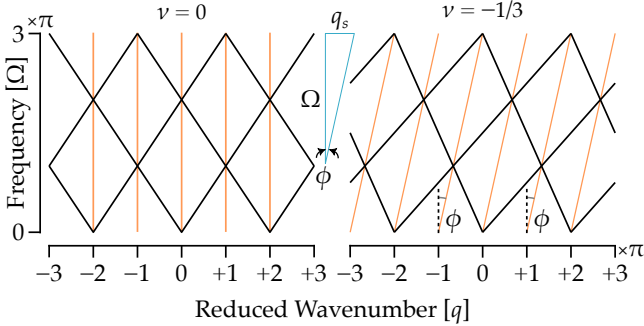


Figure 1: A comparison between reciprocal ($\nu = 0$) and non-reciprocal ($\nu = -1/3$) band structures, corresponding to the wave equation in Equation (1), having the dispersion relation in Equation (6). The definition of the skew angle ϕ can be perceived as an angle in a triangle, constructed via the wavenumber phase shift q_s and its corresponding frequency Ω . Note that the dispersion relation is repeated periodically along the wavenumber axis for better visualization of the skew angle.

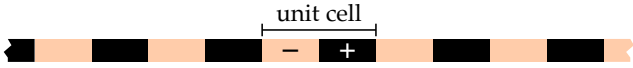


Figure 2: Schematic of an infinite elastic rod with a unit cell of alternating negative/positive Willis coupling.

Elastic rod with periodic Willis coupling

Consider a unit cell of an elastic rod divided evenly into two segments as seen in Figure 2. Each segment has equal normalized length $\xi = 1/2$, cross-sectional area, and material properties, yet reversed signs of Willis coupling. The transfer matrix for

such a unit cell can be found by multiplying the transfer matrix for each segment (i.e., Equation (3)), which results in:

$$\mathbf{T} = \mathbf{e}^{-\frac{1}{2}i(\nu_+ - \nu_-)\Omega} \mathbf{Y}(\nu_+) \mathbf{Y}(-\nu_-) \quad (8)$$

where ν_- and ν_+ denote the Willis couplings of the negative and positive segment, respectively. As inferred from Equation (8), setting $\nu_+ = \nu_- = \nu$ reduces the phase parameter $\mathbf{e}^{-\frac{1}{2}i(\nu_+ - \nu_-)\Omega}$ to one as a consequence of equal magnitude and opposite signs of Willis couplings. Although each segment is *non-reciprocal* on its own, the lack of a phase parameter renders a zero skew angle, pertaining to a *reciprocal* dispersion relation. Following identical procedure to the development of Equation (6), the driven-wave dispersion relation of an elastic rod with alternating signs of Willis coupling (and equal magnitude) is:

$$q = \pm \cos^{-1} \left(\nu^2 + (1 - \nu^2) \cos(\Omega) \right) \quad (9)$$

As expected, no phase shift in the wavenumber is observed from Equation (9). Interestingly, the proposed rod design yields *wavenumber* bandgaps when $\nu \neq 0$. At $\Omega = (2p - 1)\pi$, where $p \in \mathbb{N}$ and \mathbb{N} is the set of natural numbers, wavenumber bandgaps initiate around odd integer multiples of $q = \pm\pi$, and the gaps' width is proportional to ν 's magnitude. To observe the wavenumber bandgaps, Equation (9) solutions are repeated periodically along the wavenumber axis every 2π , necessarily generating wavenumber bandgaps of *identical* width, with their lower and upper limits, respectively, being:

$$q_- = \pm \left[2(n - 1)\pi + \cos^{-1}(2\nu^2 - 1) \right] \quad (10a)$$

$$q_+ = \pm \left[2n\pi - \cos^{-1}(2\nu^2 - 1) \right] \quad (10b)$$

Note that $n \in \mathbb{N}$ denotes the order of the wavenumber bandgap. Using Equation (10), a formula for the identical wavenumber-bandgaps' width is deduced:

$$\Delta q = 2 \left(\pi - \cos^{-1}(2\nu^2 - 1) \right) \quad (11)$$

Figure 3 shows band structure examples of a material with no Willis coupling (as the baseline) and with reversed-sign Willis couplings with $\nu = \pm 0.25$ and ± 0.5 , showing the emergence of wavenumber bandgaps as predicted by Equation (10). As can be seen, flipping the sign of ν does not affect the band structure as it results in a different choice of the unit cell. Further, complex frequencies emerge in wavenumber bandgap [28], and the magnitude of the imaginary part grows larger with higher magnitudes of ν . The dispersion analyses are verified via the finite element method (depicted as circles in the figure), which agrees excellently with the analytical predictions. For reference, the wavenumber bandgap limits q_{\pm} and corresponding width are also shown for a swept range of ν . As ν approaches the limiting case of 1, the dispersion curves become vertical lines and the wavenumber-bandgap width peaks at $\Delta q = 2\pi$.

Similarities between reversed-sign Willis couplings and bi-layered periodicity

In regard of the bandgap opening mechanism, a resemblance between reversed-sign periodicity in Willis coupling and

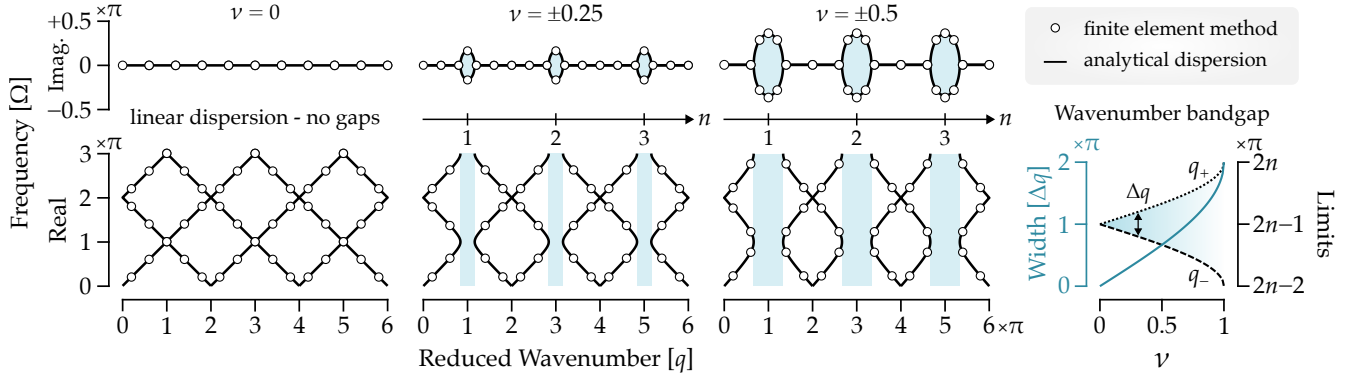


Figure 3: (left) Dispersion diagrams for the uniform rod with linear dispersion and no gaps ($\nu = 0$) and a rod with Willis coupling of alternating signs and $\nu = \pm 0.25, \pm 0.5$. As can be seen, the wavenumber bandgaps open (shaded areas) whenever $\nu \neq 0$ and grows in size with increasing its magnitude, regardless of the sign. All orders of wavenumber bandgaps (denoted by n) have identical width. Frequencies are complex within said gaps and have larger imaginary values with higher $|\nu|$. Finite element simulations (depicted as circles) provide further validation to the analytical results. (right) Wavenumber-bandgap width Δq and limits q_{\pm} as a function of ν , corroborating the behavior of bandgap growth in the dispersion diagrams.

Table 1: Comparison between the expressions for the limits and width of wavenumber bandgaps for materials with alternating signs of Willis couplings (Figure 2) and those of frequency bandgaps of a bi-layered phononic crystals with a zero frequency contrast and a non-zero impedance contrast [8].

Bandgap type	Lower limit	Upper limit	Width
Wavenumber	$q_- = 2(n-1)\pi + \cos^{-1}(2\nu^2 - 1)$	$q_+ = 2n\pi - \cos^{-1}(2\nu^2 - 1)$	$\Delta q = 2(\pi - \cos^{-1}(2\nu^2 - 1))$
Frequency	$\Omega_- = (n-1)\pi + \frac{1}{2}\cos^{-1}(2\beta^2 - 1)$	$\Omega_+ = n\pi - \frac{1}{2}\cos^{-1}(2\beta^2 - 1)$	$\Delta\Omega = \pi - \cos^{-1}(2\beta^2 - 1)$

phononic crystals of two layers (1 and 2) with special modulation parameters is noticed. It has been recently shown that identical frequency bandgaps in phononic crystals open with perfect periodicity along the frequency axis by satisfying two conditions [8]:

- A zero frequency contrast, achieved via setting $\ell_1 c_2 = \ell_2 c_1$, and
- A non-zero characteristic impedance contrast $\beta = (z_1 - z_2)/(z_1 + z_2)$, where $z_{1,2} = A_{1,2}\sqrt{E_{1,2}\rho_{1,2}}$ are the characteristic impedance of the constitutive layers².

For easier comparisons, Table 1 is compiled to concisely summarize the similarities between the alternating Willis-coupling rod design and the bi-layered phononic crystal in terms of bandgap limits and width. As inferred from the table, the functions governing the frequency-bandgap limits exhibit nearly identical resemblance to their wavenumber-bandgap counterpart, which extrapolates to the functions for the bandgaps' width. Apart from a 2 multiplier for the wavenumber bandgap equations, the two equation sets are identical as if the parameters ν and q are swapped with β and Ω , respectively. As such, one may deduce that the role of impedance contrast in opening a frequency bandgap is equivalent to the role of the normalized modulation speed ν in opening a wavenumber bandgap, given reversed-sign Willis coupling.

Concluding remarks

The introduction of Willis coupling in elastic media traditionally yields non-reciprocal band structure due the presence of mo-

mentum bias. Peculiarly, reversing Willis-coupling signs within a unit cell, *ceteris paribus*, is analytically proven to produce reciprocal band structures with wavenumber bandgaps, and analogies to a special class of bi-layered phononic crystals are noted. Future research directions of the proposed methodology could be focused on physical realizations of periodic Willis coupling. For instance, while physical motion of an elastic rod gives rise to Willis coupling, synthesizing a feedback controller (e.g., Refs.[29–31]) could be an alternative route for realizing Willis coupling, especially if a periodic variation in Willis coupling is sought.

¹M. A. Attarzadeh and M. Nouh, “Elastic wave propagation in moving phononic crystals and correlations with stationary spatiotemporally modulated systems”, *AIP Advances* **8**, 105302 (2018).

²J. A. Wickert and J. Mote C. D., “Classical Vibration Analysis of Axially Moving Continua”, *Journal of Applied Mechanics* **57**, 738–744 (1990).

³H. Nassar, X. Xu, A. Norris, and G. Huang, “Modulated phononic crystals: non-reciprocal wave propagation and willis materials”, *Journal of the Mechanics and Physics of Solids* **101**, 10–29 (2017).

⁴H. Nassar, A. N. Norris, and G. Huang, “Waves over a periodic progressive modulation: a python tutorial”, in *Acoustic metamaterials: absorption, cloaking, imaging, time-modulated media, and topological crystals*, edited by R. Craster and S. Guenneau (Springer Nature Switzerland, Cham, 2024), pp. 505–533.

⁵H. B. Al Ba’ba’a, “Brillouin-zone definition in non-reciprocal Willis monatomic lattices”, *JASA Express Letters* **3**, 120001 (2023).

⁶H. Al Ba’ba’a and M. Nouh, “An investigation of vibrational power flow in one-dimensional dissipative phononic structures”, *Journal of Vibration and Acoustics, Transactions of the ASME* **139**, 21003–21010 (2017).

²Note that all variables hold identical meaning to what has been defined in the article, and the subscripts 1 and 2 are used to distinguish the first and second layer of the bi-layered phononic crystal.

- ⁷M. I. Hussein, G. M. Hulbert, and R. A. Scott, "Dispersive elastodynamics of 1d banded materials and structures: design", *Journal of Sound and Vibration* **307**, 865–893 (2007).
- ⁸H. B. Al Ba'ba'a and M. Nouh, "The role of frequency and impedance contrasts in bandgap closing and formation patterns of axially-vibrating phononic crystals", *Journal of Applied Mechanics* **91**, 031006 (2023).
- ⁹M. G. El Sherbiny and L. Placidi, "Discrete and continuous aspects of some metamaterial elastic structures with band gaps", *Archive of Applied Mechanics* **88**, 1725–1742 (2018).
- ¹⁰L. Liu and M. I. Hussein, "Wave motion in periodic flexural beams and characterization of the transition between bragg scattering and local resonance", *Journal of Applied Mechanics* **79**, 011003 (2011).
- ¹¹M. Nouh, O. Aldraihem, and A. Baz, "Vibration characteristics of metamaterial beams with periodic local resonances", *Journal of Vibration and Acoustics, Transactions of the ASME* **136**, 61012 (2014).
- ¹²L. M. Nash, D. Kleckner, A. Read, V. Vitelli, A. M. Turner, and W. T. Irvine, "Topological mechanics of gyroscopic metamaterials", *Proceedings of the National Academy of Sciences of the United States of America* **112**, 14495–14500 (2015).
- ¹³M. Garau, G. Carta, M. J. Nieves, I. S. Jones, N. V. Movchan, and A. B. Movchan, "Interfacial waveforms in chiral lattices with gyroscopic spinners", *Proceedings of the Royal Society A: Mathematical, Physical and Engineering Sciences* **474**, 20180132 (2018).
- ¹⁴Y. Alsaffar, S. Sassi, and A. Baz, "Band gap characteristics of periodic gyroscopic systems", *Journal of Sound and Vibration* **435**, 301–322 (2018).
- ¹⁵M. Attarzadeh, S. Maleki, J. Crassidis, and M. Nouh, "Non-reciprocal wave phenomena in energy self-reliant gyric metamaterials", *The Journal of the Acoustical Society of America* **146**, 789–801 (2019).
- ¹⁶L. Placidi, F. Di Girolamo, and R. Fedele, "Variational study of a maxwell-rayleigh-type finite length model for the preliminary design of a tensegrity chain with a tunable band gap", *Mechanics Research Communications* **136**, 104255 (2024).
- ¹⁷L. Placidi, J. de Castro Motta, and F. Fraternali, "Bandgap structure of tensegrity mass-spring chains equipped with internal resonators", *Mechanics Research Communications* **137**, 104273 (2024).
- ¹⁸A. Amendola, A. Krushynska, C. Daraio, N. M. Pugno, and F. Fraternali, "Tuning frequency band gaps of tensegrity mass-spring chains with local and global prestress", *International journal of solids and structures* **155**, 47–56 (2018).
- ¹⁹A. Misra and P. Poorolajou, "Granular micromechanics based micro-morphic model predicts frequency band gaps", *Continuum Mechanics and Thermodynamics* **28**, 215–234 (2016).
- ²⁰N. NejadSadeghi and A. Misra, "Axially moving materials with granular microstructure", *International Journal of Mechanical Sciences* **161**, 105042 (2019).
- ²¹N. NejadSadeghi and A. Misra, "Role of higher-order inertia in modulating elastic wave dispersion in materials with granular microstructure", *International Journal of Mechanical Sciences* **185**, 105867 (2020).
- ²²A. Misra and N. NejadSadeghi, "Longitudinal and transverse elastic waves in 1d granular materials modeled as micromorphic continua", *Wave Motion* **90**, 175–195 (2019).
- ²³M. I. Hussein, M. J. Leamy, and M. Ruzzene, "Dynamics of phononic materials and structures: Historical origins, recent progress, and future outlook", *Applied Mechanics Reviews* **66**, 040802 (2014).
- ²⁴Y.-F. Wang, Y.-Z. Wang, B. Wu, W. Chen, and Y.-S. Wang, "Tunable and active phononic crystals and metamaterials", *Applied Mechanics Reviews* **72**, 040801 (2020).
- ²⁵Y. Jin, Y. Pennec, B. Bonello, H. Honarvar, L. Dobrzynski, B. Djafari-Rouhani, and M. I. Hussein, "Physics of surface vibrational resonances: pillared phononic crystals, metamaterials, and metasurfaces", *Reports on Progress in Physics* **84**, 086502 (2021).
- ²⁶M. I. Hussein and M. J. Frazier, "Band structure of phononic crystals with general damping", *Journal of Applied Physics* **108** (2010).
- ²⁷G. Trainiti, Y. Xia, J. Marconi, G. Cazzulani, A. Erturk, and M. Ruzzene, "Time-Periodic Stiffness Modulation in Elastic Metamaterials for Selective Wave Filtering: Theory and Experiment", *Physical Review Letters* **122**, 124301 (2019).
- ²⁸M. Moghaddasadeh, M. Attarzadeh, A. Aref, and M. Nouh, "Complex spatiotemporal modulations and non-hermitian degeneracies in \mathcal{PT} -symmetric phononic materials", *Phys. Rev. Appl.* **18**, 044013 (2022).
- ²⁹J. E. Pechac and M. J. Frazier, "Non-reciprocal supratransmission in mechanical lattices with non-local feedback control interactions", *Crystals* **11**, 94 (2021).
- ³⁰M. I. N. Rosa and M. Ruzzene, "Dynamics and topology of non-hermitian elastic lattices with non-local feedback control interactions", *New Journal of Physics* **22**, 053004 (2020).
- ³¹H. Alli and T. Singh, "On the feedback control of the wave equation", *Journal of Sound and Vibration* **234**, 625–640 (2000).